Supporting Information

Dual-Function Ni-based MOF for Hydrogen Storage and CO_2 to Carbonate Cyclic Catalysis

Elena García-Rojas,[a] Helena Montes-Andrés,[a] Jesús Tapiador,[a] Carmen Martos,[a] Pablo Salcedo-Abraira,[b] Duane Choquesillo-Lazarte,[c] Gisela Orcajo[a], Pedro Leo[a*]*

[a] Chemical and Environmental Engineering Group, ESCET, Universidad Rey Juan Carlos. C/ Tulipán s/n 28933, Móstoles (Spain).
[b] Department of Inorganic Chemistry, University of Granada, Avda. Fuentenueva s/n, Granada (Spain).
[c] Laboratorio de Estudios Cristalográficos, IACT, CSIC-Universidad de Granada, Avda. de las Palmeras 4, 18100 Armilla, Granada, Spain.

Synthesis of 5,5'-(diazene-1,2-diyl)diisophthalic acid ligand [H_4ABTC]

Dissolve 5-nitroisophthalic acid (5 g, 23.7 mmol) in NaOH (6.6 g, 0.165 mol) and 70 mL H_2O into a two-neck flask at 60 °C. The mixture turns a light pink color and is maintained at this temperature and with vigorous stirring for 1 h. After this time, a solution of glucose (13.16 g, 73.04 mmol) in water (40 mL) is added dropwise until the reaction mixture turns dark brown. After complete addition of the glucose solution, the reaction mixture is removed from the heating to room temperature and, under stirring, a positive stream of air is passed through for 16 h. The reaction mixture is then cooled in an ice bath and the acid salt H_4ABTC is recovered by filtration. The solid is dissolved in 120 mL of distilled water and HCl is added dropwise until pH = 1. The precipitate is filtered, washed repeatedly with water and recrystallized in DMF, yielding a bright orange solid (yield: 79%, 6.7 g). ^{1}H NMR (400 MHz, $CDCl_3$): δ = 8.60 (t, J = 1.6 Hz, 2H), 8.57 (d, J = 1.6 Hz, 4H).

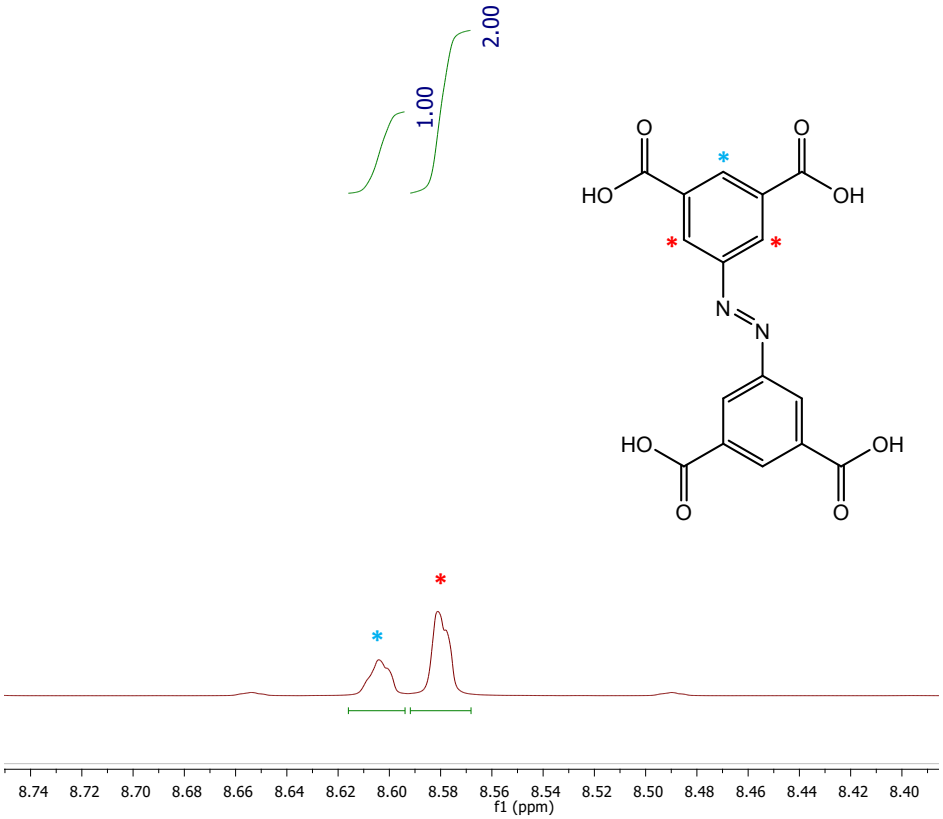

Figure S1. ^{1}H-NMR (400 MHz, DMSO, 298 K) of H_4ABTC.

Table S1. Crystal data and structure refinement for Ni-URJC-3.

Identification code	Ni-URJC-3
Empirical formula	$C_{32.7}H_{39.8}N_{7.6}Ni_2O_{13.6}$
Formula weight	872.64
Temperature/K	150.00
Crystal system	tetragonal
Space group	$P4_12_12$
a/Å	13.7192(12)
b/Å	13.7192(12)
c/Å	45.094(4)
α/°	90
β/°	90
γ/°	90
Volume/Å^3	8487.5(17)
Z	8
ρ_{calc}g/cm^3	1.366
μ/mm^{-1}	0.955
F(000)	3625.0
Crystal size/mm^3	0.08 × 0.07 × 0.04
Radiation	MoKα (λ = 0.71073)
2Θ range for data collection/°	5.54 to 50.08
Index ranges	-16 ≤ h ≤ 13, -16 ≤ k ≤ 15, -51 ≤ l ≤ 51
Reflections collected	40553
Independent reflections	7246 [R_{int} = 0.1312, R_{sigma} = 0.1518]
Data/restraints/parameters	7246/875/583
Goodness-of-fit on F^2	1.217
Final R indexes [I>=2σ (I)]	R_1 = 0.1260, wR_2 = 0.2420
Final R indexes [all data]	R_1 = 0.1711, wR_2 = 0.2568
Largest diff. peak/hole / e Å^{-3}	1.00/-1.06
Flack parameter	0.50(7)

Table S2. Selected Bond Lengths for Ni-URJC-3

Atom	Atom	Length/Å

Atom	Atom	Length/Å
Ni2	O1	2.068(8)
Ni2	O3	2.172(9)
Ni2	O11[1]	2.090(8)
Ni2	O14	1.988(8)
Ni2	O25[2]	2.019(9)
Ni2	O12[1]	2.155(8)
Ni1	O1	2.074(9)
Ni1	O32	2.080(9)
Ni1	O27	2.093(10)
Ni1	O15	2.017(9)
Ni1	O24[2]	2.030(9)
Ni1	O37	2.043(9)
N20	N20[3]	1.26(2)

[1]1/2+X,1/2-Y,3/4-Z; [2]1/2+X,3/2-Y,3/4-Z; [3]+Y, +X,1-Z; [4]1-Y,1-X,1/2-Z

a)

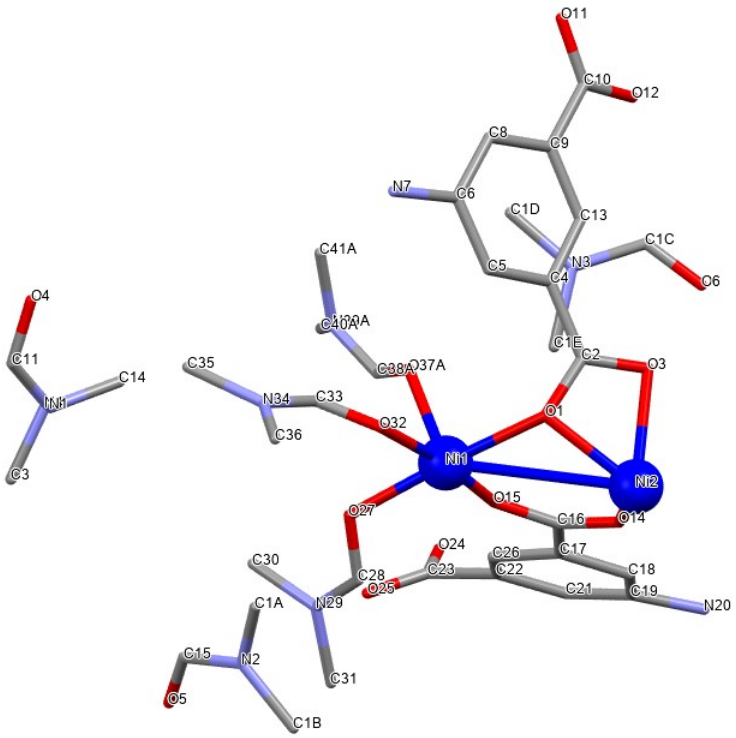

b)

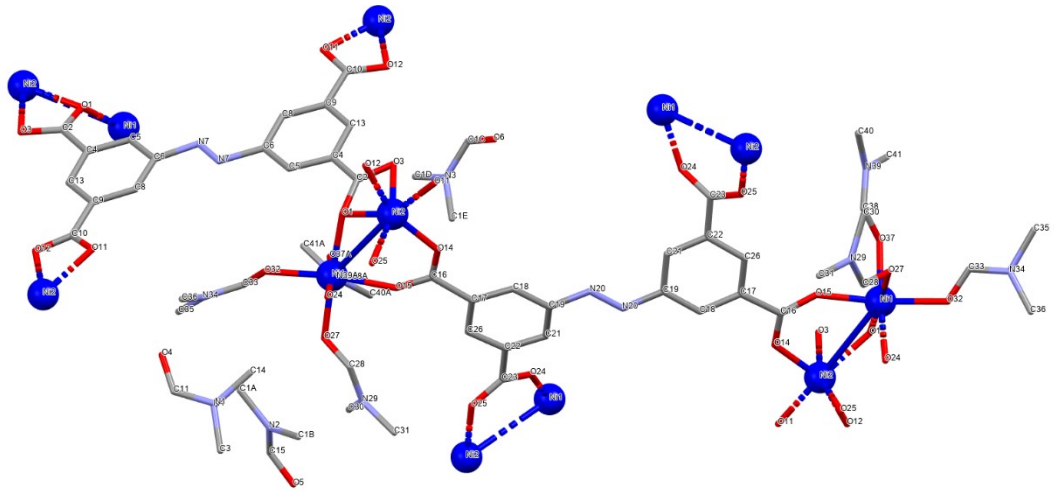

Figure S2. Detailed crystal structure of Ni-URJC-3 showing atom labeling and coordination geometry of a) the Ni_2O_{11} secondary building unit, b) as well as the connection of $ABTC^{-4}$ ligands forming the 3D porous framework. Colour code: Ni in dark blue, nitrogen in light blue, oxygens in red and carbons in grey. Hydrogen and solvated DMF were removed for clarity.

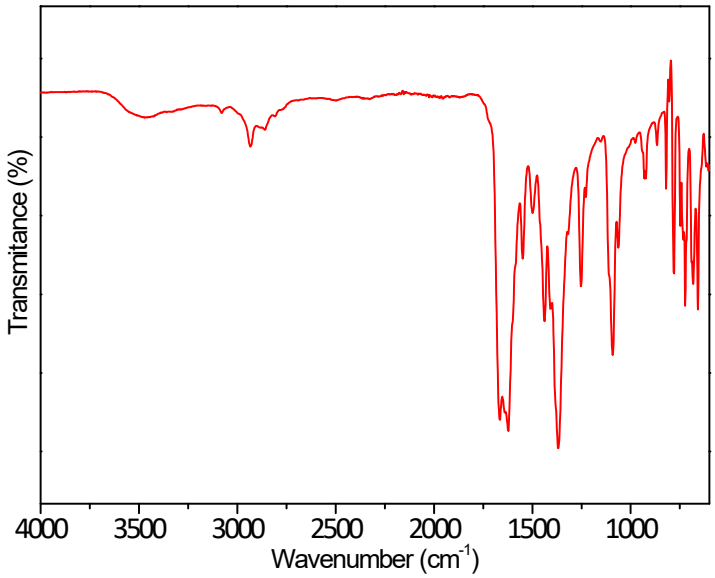

Figure S3. FTIR of the Ni-URJC-3 material after degassing at 120 °C for 12 hours under vacuum.

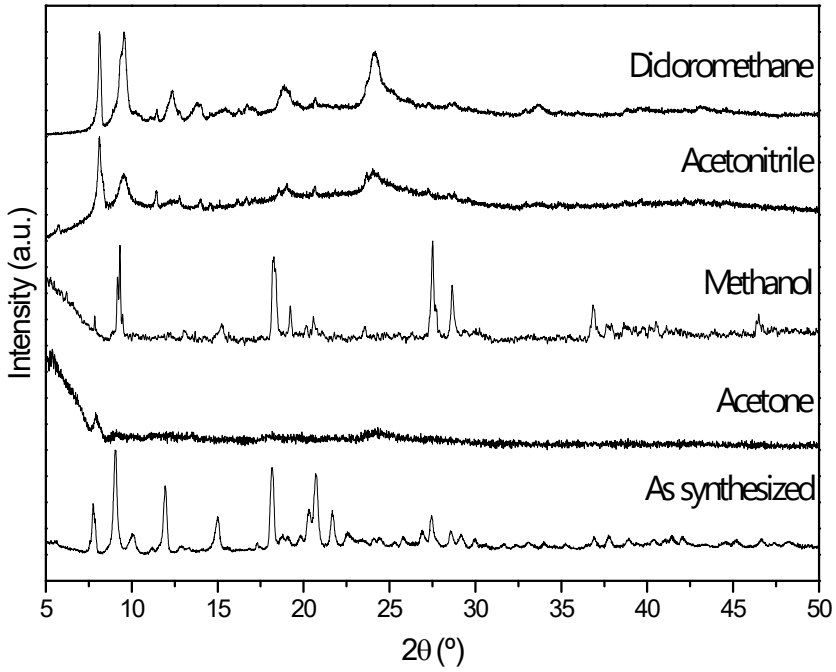

Figure S4. XRD of the Ni-URJC-3 material after solvent-exchange stability tests in methanol, acetone, acetonitrile and dichloromethane.

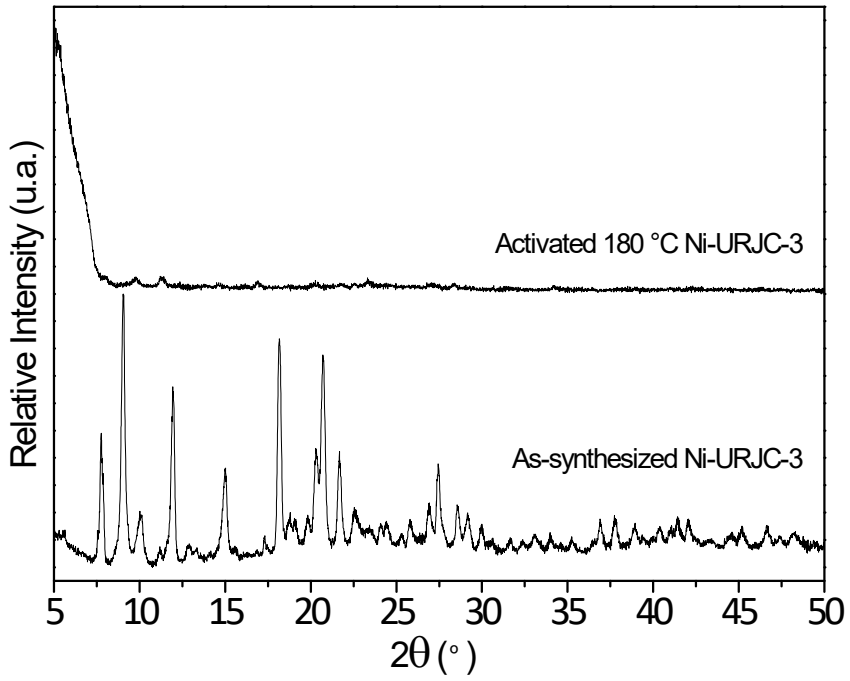

Figure S5. XRD of the Ni-URJC-3 material subjected to a heat treatment of 180 °C compared to the synthesised material.

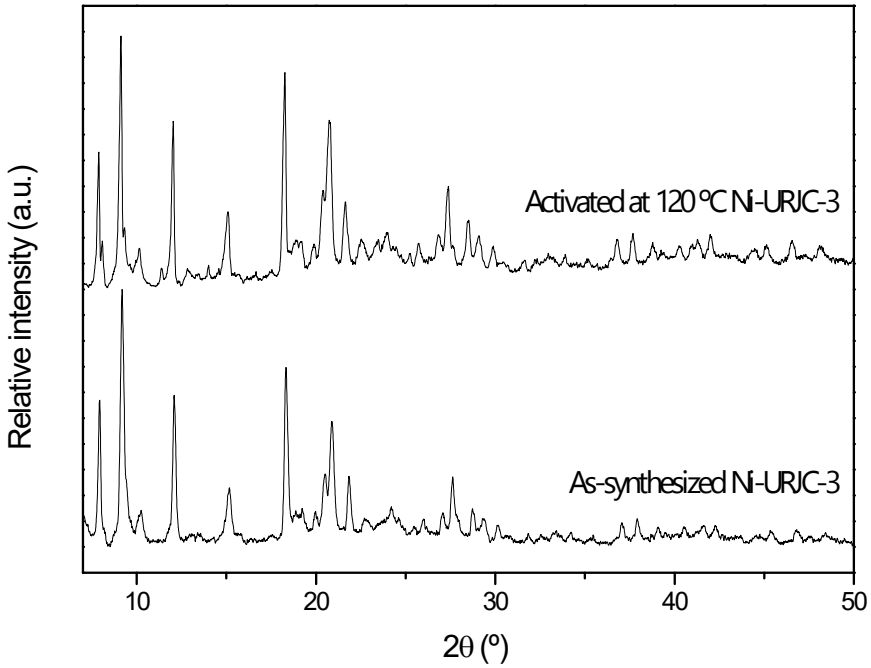

Figure S6. XRD of the Ni-URJC-3 material subjected to a heat treatment of 120 °C compared to the synthesized material.

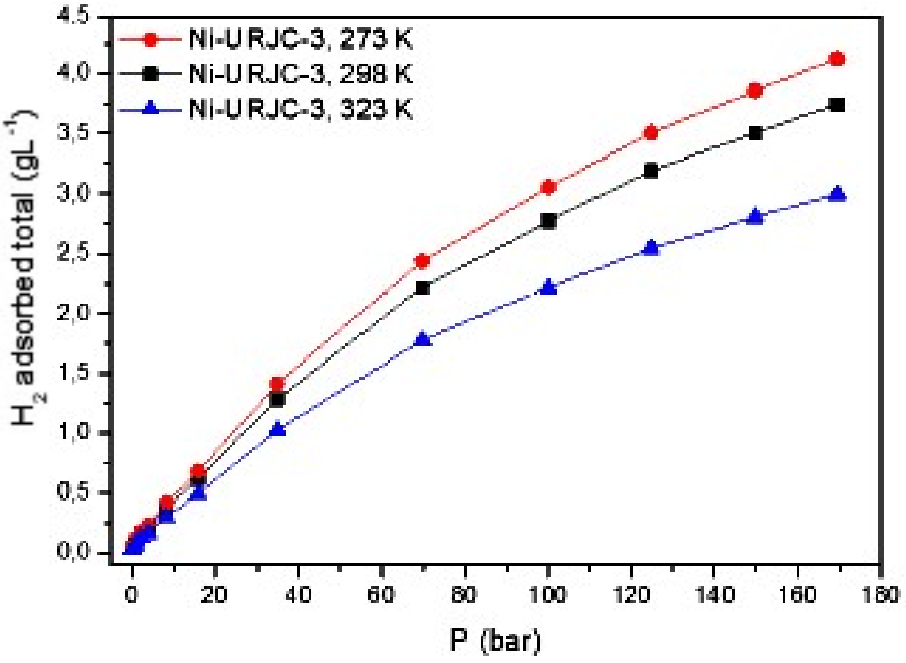

Figure S7. Adsorption isotherm of H_2 at temperatures 273, 298 and 323 K.

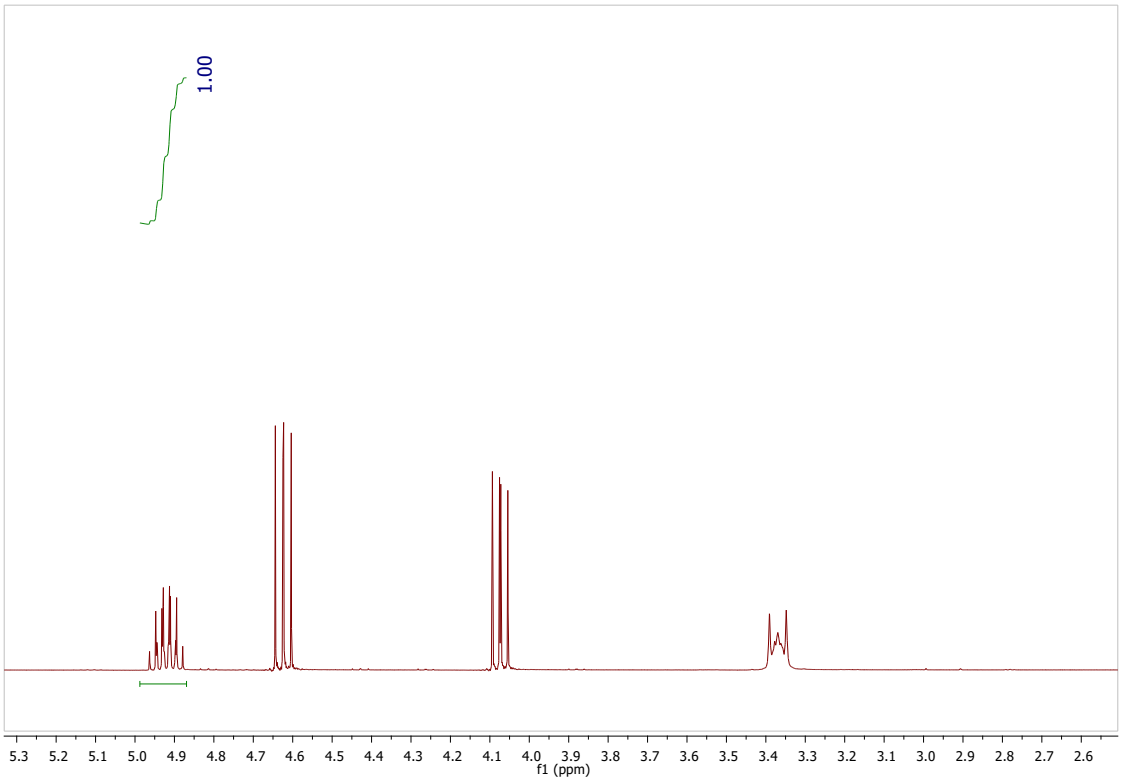

Figure S8. Signal integration in H-NMR plot for reactions with propylene oxide.

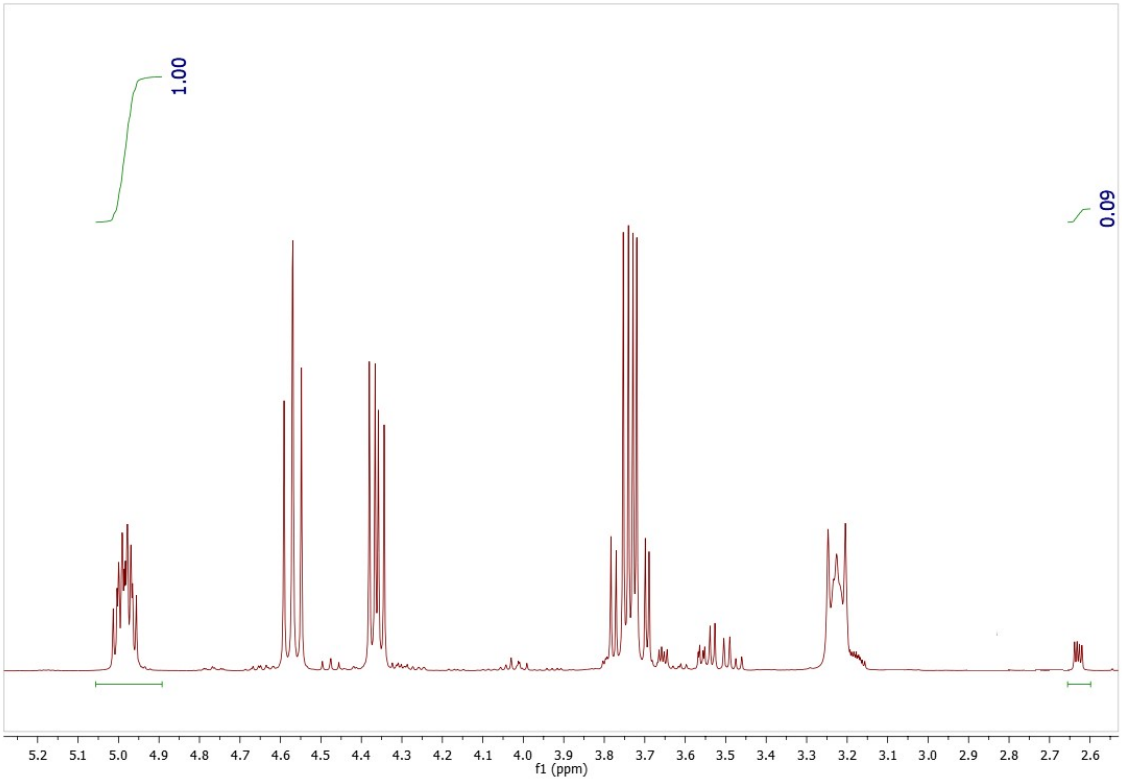

Figure S9. Signal integration in H-NMR plot for reactions with epichlorohydrin.

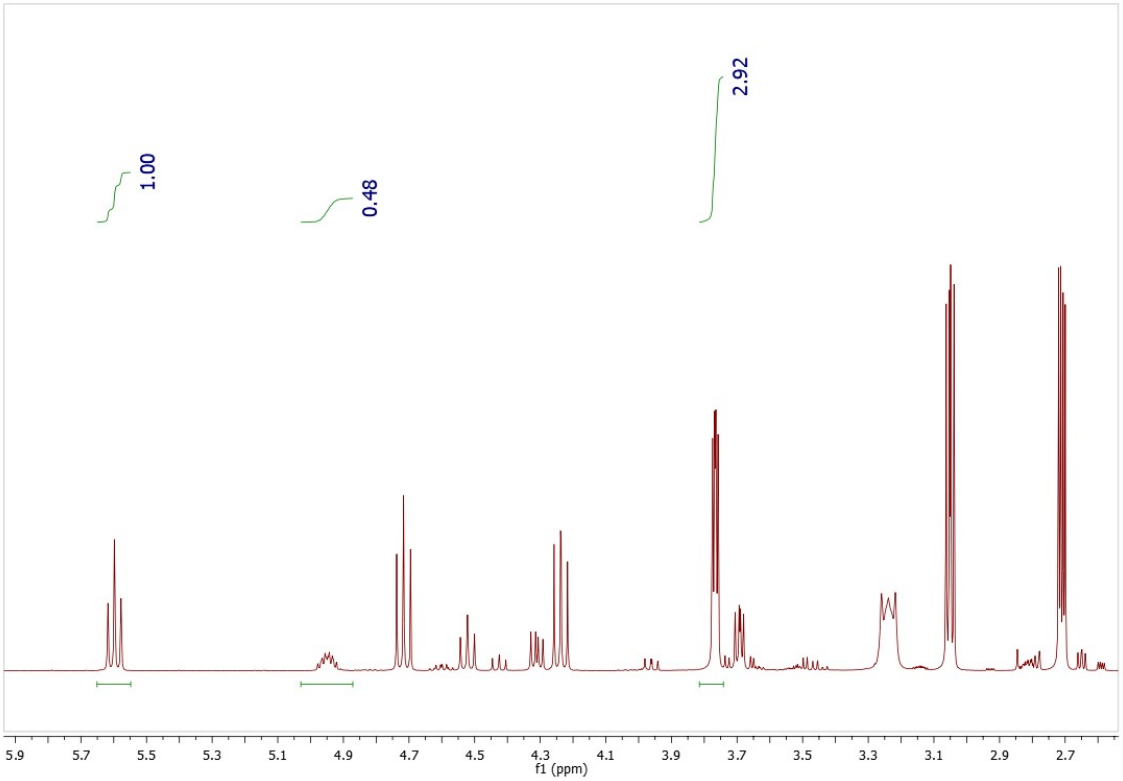

Figure S10. Signal integration in H-NMR plot for reactions with styrene oxide.

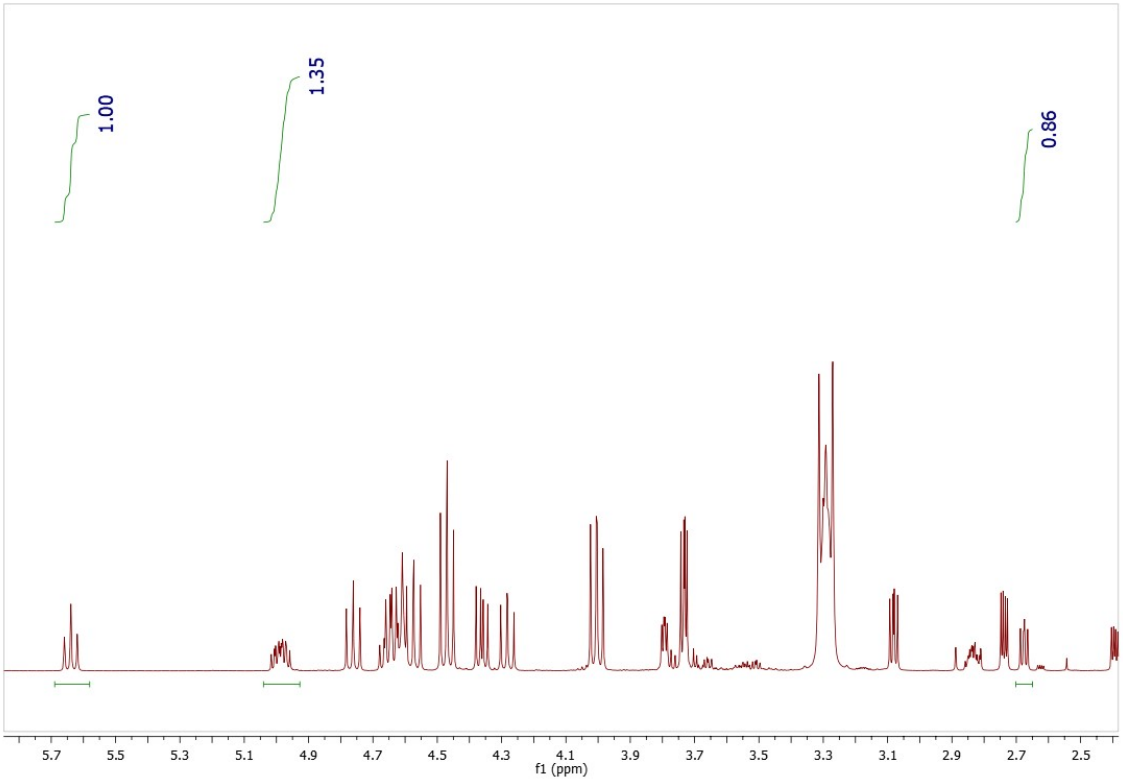

Figure S11. Signal integration in H-NMR plot for reactions with 1,2-epoxihexane.

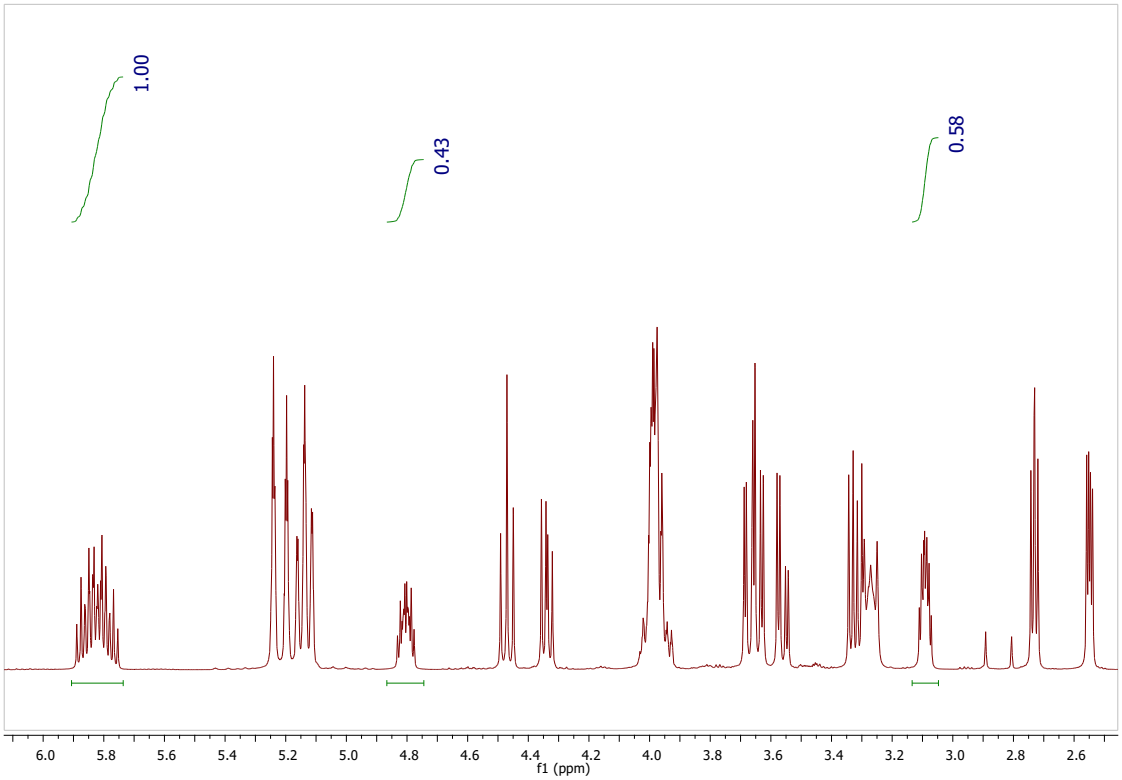

Figure S12. Signal integration in H-NMR plot for reactions with Allyl glycidyl ether.

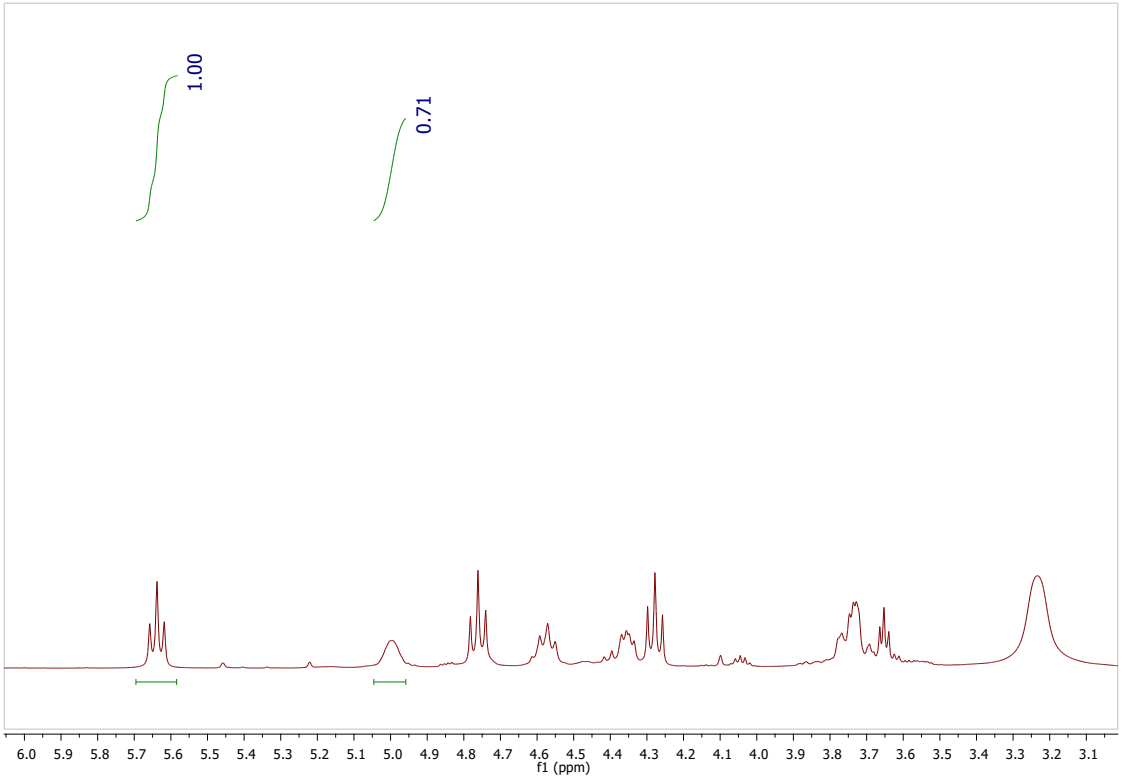

Figure S13. Signal integration in H-NMR plot for reactions with styrene oxide at 80 °C.

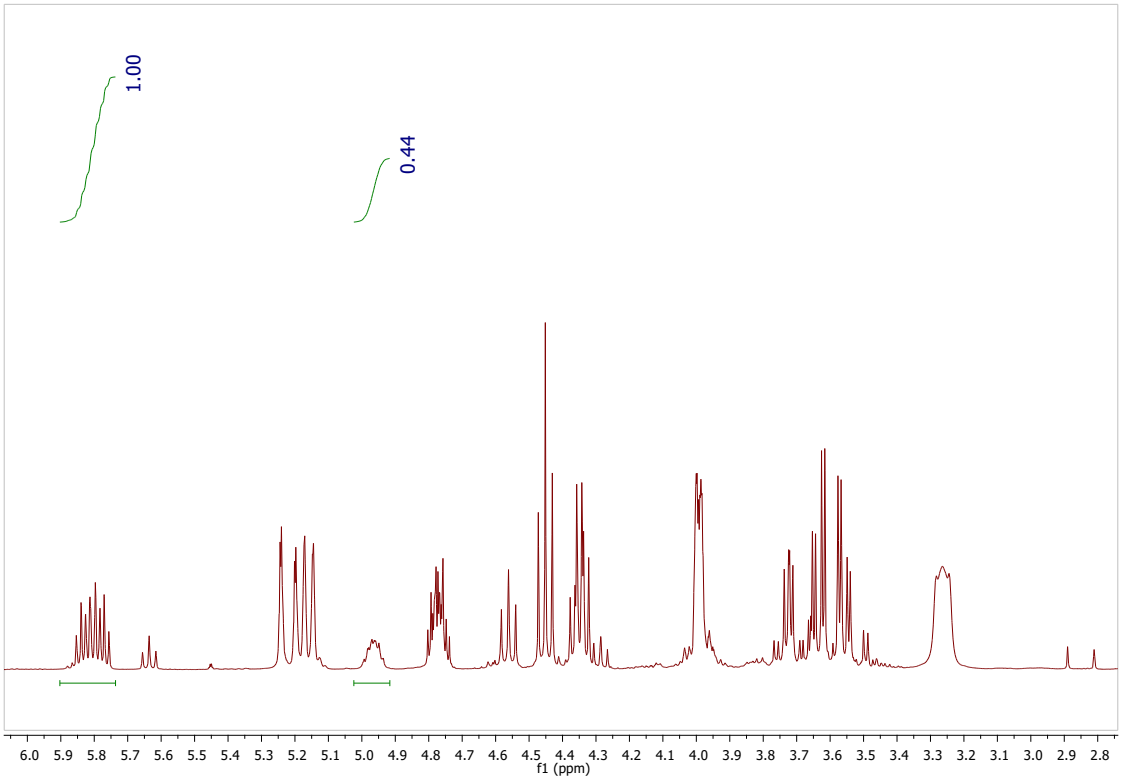

Figure S14. Signal integration in H-NMR plot for reactions with Allyl glycidyl ether at 80 °C.

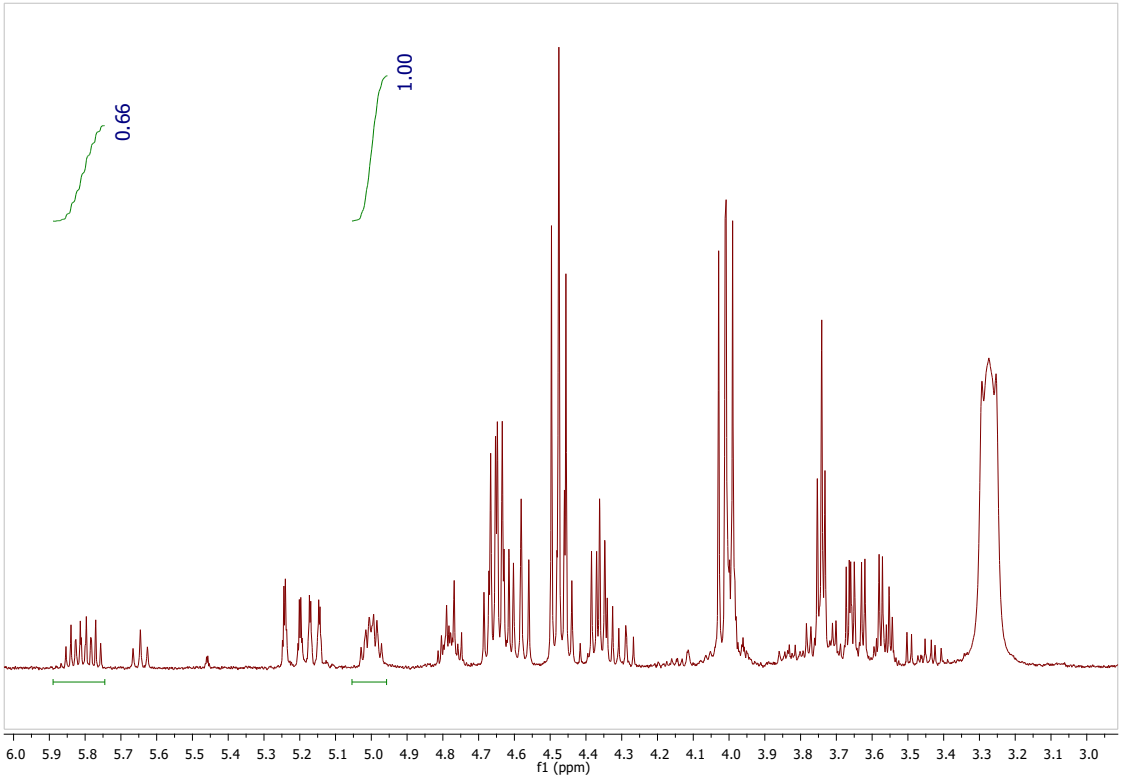

Figure S15. Signal integration in H-NMR plot for reactions with 1,2-epoxihexane at 80 °C.